ChemCatChem
Research Article
doi.org/10.1002/cctc.202401172
Chemistry Europe
European Chemical Societies Publishing
www.chemcatchem.org

Hydrogenation of Alkenes Catalyzed by Mn(I) Alkyl Complexes Bearing NHC Phosphine Ligands

Daniel P. Zobernig,[a] Berthold Stöger,[b] Luis F. Veiros,[c] and Karl Kirchner*[a]

This paper is dedicated to Prof. Anna M. Trzeciak on occasion of her 70th birthday.

An efficient additive free hydrogenation of alkenes with molecular hydrogen is described. The pre-catalyst is a well-defined bench stable Mn(I) alkyl complex bearing a NHC phosphine ligand. These reactions are environmentally benign and atom economic, implementing an inexpensive, earth abundant non-precious metal catalyst. The catalytic process is initiated by migratory insertion of a CO ligand into the Mn-alkyl bond to yield an acyl intermediate which undergoes rapid hydrogenolysis to form the active 16e Mn(I) hydride catalyst [Mn(PC-*i*Pr)(CO)$_2$(H)]. A range of mono- and disubstituted alkenes were efficiently converted into alkanes in good to excellent yields. The hydrogenation requires a reaction temperature of 60 °C. In all cases, a catalyst loading of 1 mol % and a hydrogen pressure of 50 bar was applied. A mechanism based on DFT calculations is presented which is supported by experimental studies.

Introduction

One of the most important research goals in organic chemistry is developing synthetic methods to obtain target molecules efficiently and selectively. However, as sustainability is of increasing importance, performing these reactions under catalytic conditions utilizing mostly earth abundant non-precious catalysts is pivotal.[1] Iron and manganese have herein been proven to be promising candidates as they are not only abundant in the Earth's crust, but also inexpensive, non-toxic and environmentally benign. In this context, the hydrogenation of olefins, alkynes, carbonyl compounds and nitriles to obtain valuable products is essential and needs to be performed as atom-efficient and cleanly as possible.[2,3]

In particular, iron, cobalt and nickel catalysts have been extensively investigated over the last years for various hydrogenation reactions.[4–9] Low valent manganese(I) catalysts have first appeared in 2016 and have been proven to be powerful players in this field.[10,11]

Mn(I) complexes were also found to be active for the hydrogenation of non-polar unsaturated bonds such as olefins (Scheme 1).[11c,12–15] Inspired by these recent discoveries of manganese catalyzed (de)hydrogenation and hydrofunctionalization reactions, we describe the synthesis of a N-heterocyclic carbene-based alkyl Mn(I) complex and its application in the efficient additive-free hydrogenation of alkenes.

Results and Discussion

The new alkyl Mn(I) complex *fac*-[Mn(PC-*i*Pr)(CO)$_3$(CH$_2$CH$_2$CH$_3$)] (**2**) was obtained by treatment of *fac*-[Mn(PC-*i*Pr)(CO)$_3$Br] (**1**) with Na (3 equiv) and subsequent addition of CH$_3$CH$_2$CH$_2$Br in 73 % isolated yield (Scheme 2). The alkyl complex is bench-stable for at least 1 week in the presence of air. It was fully characterized by ^{1}H, ^{13}C{^{1}H} and ^{31}P{^{1}H} NMR and IR spectroscopy, and high-resolution mass spectrometry. In addition, the molecular structure was determined by X-ray crystallography. A structural view is depicted in Scheme 2 with selected bond distances and angles given in the caption.

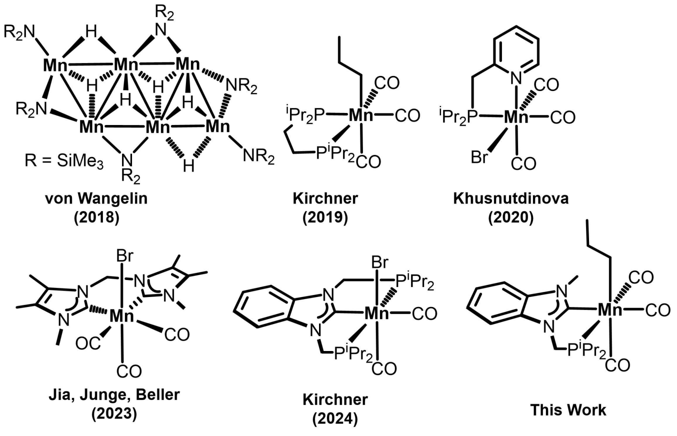

Scheme 1. Manganese Catalysts for the Hydrogenation of Alkenes.

---

[a] D. P. Zobernig, Prof. Dr. K. Kirchner
Institute of Applied Synthetic Chemistry, TU Wien, Getreidemarkt 9/163-AC, A-1060 Wien, Austria
E-mail: karl.kirchner@tuwien.ac.at

[b] Dr. B. Stöger
X-Ray Center, TU Wien, Getreidemarkt 9/163-AC, A-1060 Wien, Austria

[c] Prof. Dr. L. F. Veiros
Centro de Química Estrutural, Institute of Molecular Sciences, Departamento de Engenharia Química, Instituto Superior Técnico, Universidade de Lisboa, Av. Rovisco Pais, 1049 001 Lisboa, Portugal

Supporting information for this article is available on the WWW under https://doi.org/10.1002/cctc.202401172

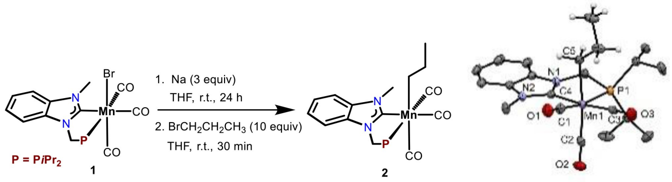

Scheme 2. Synthesis of *fac*-[Mn(PC-*i*Pr)$(CO)_3(CH_2CH_2CH_3)$] (**2**) and Structural View of **2** showing 50% Ellipsoids (H Atoms Omitted for Clarity). [a] Selected bond distances (Å) and angles (°): Mn1-C2 1.796(2), Mn1-C1 1.799(2), Mn1-C3 1.810(2), Mn1-C4 2.026(2), Mn1-C5 2.180(2), Mn1-P1 2.3053(8), C3-Mn1-C4 172.76(9), C2-Mn1-C5 173.75(9), C1-Mn1-P1 169.87(8).

The catalytic performance of complex **2** was then investigated for the hydrogenation of 4-chlorostyrene as model substrate. We tested the influence of various solvents, temperatures, and pressures. Optimization experiments are depicted in Table 1. With a catalyst loading of 1 mol% at 50 °C and a hydrogen pressure of 25 bar in THF for 18 h, 1-chloro-4-ethylbenzene was obtained in 47% yield (Table 1, entry 1). Under the same reaction conditions in the solvents toluene, $ClCH_2CH_2Cl$, and MeOH very low or no yields were achieved (Table 1, entries 2–4). Upon increasing the hydrogen pressure to 50 bar and a reaction time of 24 h, 1-chloro-4-ethylbenzene was obtained 95% yield (Table 1, entry 5). At 60 °C under the same conditions 1-chloro-4-ethylbenzene was formed in essentially quantitative yield (Table 1, entry 6). The homogeneity of the system was confirmed upon addition of one drop of mercury, whereas no decrease of reactivity and selectivity was observed. In presence of 1 equiv. of PEt_3 (with respect to substrate), only traces of product formation could be detected, which indicates an inner-sphere mechanism, due to coordination of PEt_3 at a vacant side of the active species.

Table 2. Hydrogenation of Alkenes catalyzed by **2.**[a]

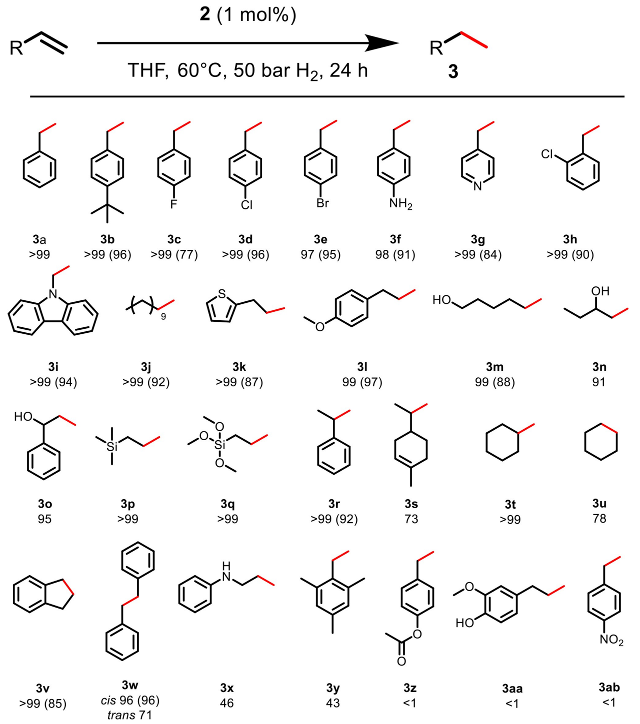

3a	>99
3b	>99 (96)
3c	>99 (77)
3d	>99 (96)
3e	97 (95)
3f	98 (91)
3g	>99 (84)
3h	>99 (90)
3i	>99 (94)
3j	>99 (92)
3k	>99 (87)
3l	99 (97)
3m	99 (88)
3n	91
3o	95
3p	>99
3q	>99
3r	>99 (92)
3s	73
3t	>99
3u	78
3v	>99 (85)
3w	*cis* 96 (96) *trans* 71
3x	46
3y	43
3z	<1
3aa	<1
3ab	<1

[a] Reaction conditions: alkene (0.5 mmol, 1 equiv), **2** (1 mol%), 0.5 mL THF, 60 °C, 50 bar H_2, 24 h, yield determined by GC-MS, isolated yields in parentheses.

Having established the best reaction conditions, various substrates have been tested to establish scope and limitations (Table 2). A variety of monosubstituted alkenes, 1,1-disubstituted alkenes and *cis*- and *trans*-1,2-disubstituted alkenes were hydrogenated affording the respective alkanes in good to high yields. Tri- and tetrasubstituted alkenes could not be hydrogenated. The catalytic protocol shows high functional group tolerance, halides, amino and hydroxy groups, and ethers were well tolerated. A number of aromatic terminal alkenes bearing electron-withdrawing and electron-donating groups in the *para*-position were successfully converted into the corresponding alkanes with excellent yields (**3a**–**3e**). Styrene derivatives bearing nitrogen containing functionalities such as 4-vinylaniline and 4-vinylpyridine could also be hydrogenated with no drop in reactivity (**3f**, **3g**). Sterically more hindered 2-chlorostyrene was also fully reacted to 1-chloro-2-ethylbenzene, same as N-Vinylcarbazole (**3h**, **3i**). Aliphatic alkenes bearing thiophene or methoxy moieties were successfully hydrogenated (**3j**–**3l**). Also hydroxy groups were tolerated and with the respective alkanes being formed in high yields (**3m**–**3o**). Allyltrimethylsilane and allyltrimethoxysilane were also fully converted into the corresponding alkanes (**3p**, **3q**). In addition, 1,1-disubstitued alkenes could be hydrogenated albeit with somewhat lower yields (**3r**–**3u**). In the case of **3s**, only the terminal double bond was hydrogenated. Complete hydrogenation of internal alkenes such as *trans*- and *cis*-stilbenes (**3w**) and cyclic substrates such as 1*H*-indene (**3v**) were also achieved. N-Allylaniline (**3x**) exhibited only moderate yield, same as the electron-rich 2,4,6-trimethylstyrene (**3y**). On the other hand, in the presence of ester-, phenol-, and nitro-groups the catalyst was inactive with no conversion being observed (**3z**–**3ab**).

Table 1. Optimization of the Reaction Conditions for the Hydrogenation of 4-Chlorostyrene.[a]

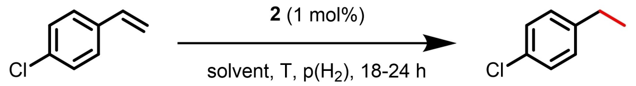

entry	Pressure (bar)	Solvent	T (°C)	T (h)	Yield (%)
1	25	THF	50	18	47
2	25	toluene	50	18	16
3	25	$ClCH_2CH_2Cl$	50	18	15
4	25	MeOH	50	18	–
5	50	THF	50	24	95
6	50	THF	60	24	>99

[a] Reaction conditions: 4-Chlorostyrene (60 μL, 0.5 mmol, 1 equiv), **2** (2.2 mg, 5 μmol, 1 mol%), 0.5 mL solvent, 50–60 °C, 25–50 bar H_2,18–24 h, yield determined by GC-MS.

Table 3. Hydrogenation of Alkenes catalyzed by **4.**[a]

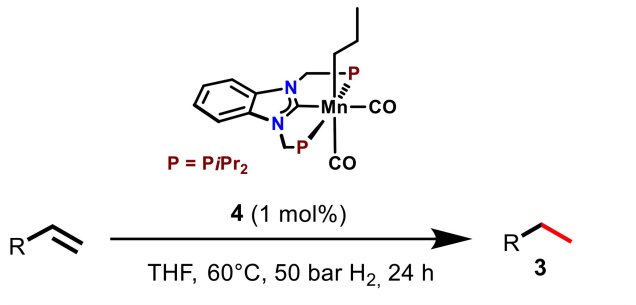

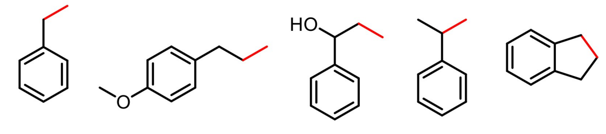

3a	**3l**	**3o**	**3r**	**3u**
>99	98	99	30	3

[a] Reaction conditions: alkene (0.5 mmol, 1 equiv), **4**(1 mol%), 0.5 mL THF, 60 °C, 50 bar H$_2$, 24 h, yield determined by GC-MS.

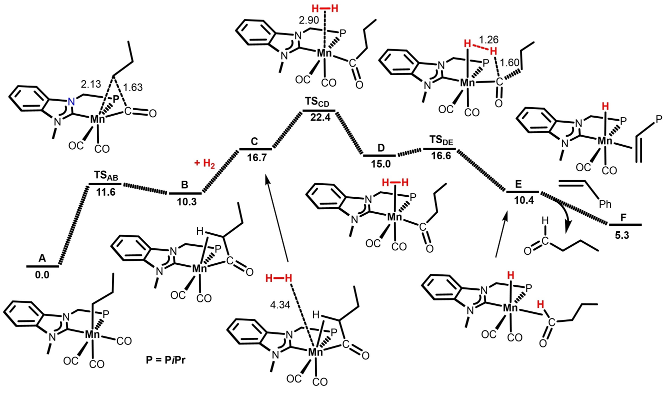

Figure 1. Free Energy Profile Calculated for the Formation and Hydrogenolysis of an Acyl Intermediate. Free Energies (kcal/mol) are Referred to *fac*-[Mn(PC-*i*Pr)(CO)$_3$(CH$_2$CH$_2$CH$_3$)] (**2**) (**A** in the calculations).

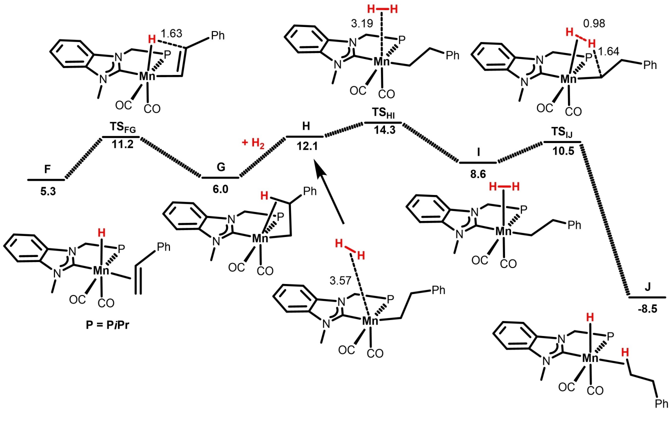

Figure 2. Free Energy Profile Calculated for the Hydrogenation of Propene. Free Energies (kcal/mol) are Referred to *fac*-[Mn(PC-*i*Pr)(CO)$_3$(CH$_2$CH$_2$CH$_3$)] (**2**) (**A** in the calculations).

For comparison, we also tested the alkyl Mn(I) complex *cis*-[Mn(PCP-*i*Pr)(CO)$_2$(CH$_2$CH$_2$CH$_3$) (**4**)[16] bearing a tridendate PCP pincer ligand as a catalyst for the hydrogenation of alkenes (Table 3). As terminal alkenes are concerned the activity of this catalyst is similar to **2** with conversions of 99, 98 and 99%, respectively, for styrene, 4-allylanisole and α-vinylbenzylalcohol (**3a**, **3l**, **3o**). With 1,1-disubstituted and 1,2-disubstituted alkenes such as α-methylstyrene (**3r**) or 1*H*-indene (**3v**) the conversion dropped drastically to 30 and 3%, respectively. This effect may be attributed to the more sterically demanding tridentate PCP-*i*Pr ligand which makes coordination of disubstituted alkenes more difficult.

The reaction mechanism was explored in detail by means of DFT calculations,[17] with styrene taken as substrate and **2** (**A** in the calculations) as pre-catalyst. The free energy profiles obtained are depicted in Figures 1 and 2. The free energy profile for the initiation process, where the active catalyst is formed, is depicted in Figure 1. The first step is the migration of the CH$_2$CH$_2$CH$_3$ ligand in complex **A** to the carbonyl C-atom of an adjacent CO ligand. This occurs in an easy step with a barrier of only 11.6 kcal/mol producing intermediate **B**, an acyl species stabilized by an agostic C–H bond. Addition of dihydrogen affords complex **D** bearing a κ^2-H$_2$ ligand. Coordination of H$_2$ has a barrier of 5.7 kcal/mol from the pair of molecules in **C** to **TS$_{CD}$** and a free energy balance of $\Delta G = -1.7$ kcal/mol, to the dihydrogen complex **D**. Finally, H-atom transfer from dihydrogen to the C-atom of the acyl ligand produces **E**, a C–H σ-complex of butanal. This last step has a barrier of only 1.6 kcal/mol and is exergonic with $\Delta G = -4.6$ kcal/mol. The catalytically active species **F** results from ligand exchange from butanal to one molecule of styrene which is thermodynamically very favorable with $\Delta G = -5.1$ kcal/mol. Experimentally, *n*-BuOH was detected by ^{1}H and ^{13}C{^{1}H} NMR spectroscopy (see ESI, Figures S2 and S3) as *n*-butanal is hydrogenated under the reaction conditions.

The free energy profile calculated for the catalytic reaction is depicted in Figure 2. Starting point is the hydride olefin complex **F** which is the active species of the catalytic reaction. In the first step of the reaction the hydride migrates to the internal olefin C-atom resulting in an alkyl complex stabilized by a C–H agostic interaction in intermediate **G**. This is a facile step with a barrier of 5.9 kcal/mol and a free energy balance of $\Delta G = 0.7$ kcal/mol. The following step corresponds to dihydrogen coordination restoring a saturated coordination environment around the metal in intermediate **I**. The overall barrier for H$_2$ coordination from intermediate **G** to the dihydrogen complex **I** is 8.3 kcal/mol, going over the less stable transition state along the path, **TS$_{HI}$**, 14.3 kcal/mol above the separated reactants. In the last step of the mechanism H-atom transfer from the dihydrogen ligand to the alkyl C-atom (a formal protonation) regenerates a hydride and forms the final product ethylbenzene that remains weakly coordinated as a C–H σ-ligand in intermediate **J**. This last step has negligible barrier (1.9 kcal/mol) and is strongly exergonic with $\Delta G = -17.1$ kcal/mol. Closing of the catalytic cycle brings **J** back to **F** with liberation of propane and coordination of a new styrene molecule in a favorable process with $\Delta G = -11.4$ kcal/mol. The overall barrier for the catalytic cycle is $\Delta G^{\ddagger} = 9.0$ kcal/mol, measured from **F**, the hydride/styrene complex, to $\mathbf{TS_{HI}}$, the transition state for H_2 coordination.

Conclusions

In sum, an efficient additive-free manganese-catalyzed hydrogenation of alkenes to alkanes with molecular hydrogen is described. The most efficient pre-catalyst is the alkyl Mn(I) complex *fac*-[Mn(PC-*i*Pr)$(CO)_3(CH_2CH_2CH_3)$] which is air-stable for several weeks in the solid state. The catalytic process is initiated by migratory insertion of a CO ligand into the Mn-alkyl bond to yield an acyl intermediate which undergoes rapid hydrogenolysis to form the active 16e$^-$ Mn(I) hydride catalyst [Mn(PC-*i*Pr)$(CO)_2$(H)]. We were able to hydrogenate a range of mono- and disubstituted alkenes to afford alkanes in good to excellent yields with high functional group tolerance. The hydrogenation of both monosubstituted, 1,1-disubstituted and 1,2-disubstituted alkenes requires a reaction temperature of 60 °C. In all cases, a catalyst loading of 1 mol % and a hydrogen pressure of 60 bar was applied. DFT calculations disclosed a typical *inner shell* mechanism with all reacting fragments coordinated to the metal. The path involves protonation of the internal C=C carbon atom followed by hydride insertion into the Mn–C bond of the resulting alkyl. In comparison to the previously reported olefin hydrogenation pre-catalyst *fac*-[Mn(dippe)$(CO)_3(CH_2CH_2CH_3)$],[11c] the present pre-catalyst *fac*-[Mn(PC-*i*Pr)$(CO)_3(CH_2CH_2CH_3)$] exhibits similar reactivities. In fact, the electron donating properties of both bidentate ligands are very similar based on their almost identical ν_{CO} stretching frequencies (see supporting information).

Experimental Section

General Information. All reactions were performed under an inert atmosphere of argon by using Schlenk techniques or in a MBraun inert-gas glovebox. The solvents were purified according to standard procedures. All alkene-substrates were purchased from Sigma-Aldrich, Acros Organics, TCI or BLDpharm and used as purchased without further purification. Complex *cis*-[Mn(PCP-*i*Pr)$(CO)_2(CH_2CH_2CH_3)$] (**4**) was synthesized according to literature.[16]

The deuterated solvents were purchased from Eurisotope and dried over 3 Å molecular sieves. ^{1}H, ^{13}C{^{1}H} and ^{31}P{^{1}H} NMR spectra were recorded on Bruker AVANCE-400 and AVANCE-600 spectrometers. ^{1}H and ^{13}C{^{1}H} NMR spectra were referenced internally to residual protio-solvent, and solvent resonances, respectively, and are reported relative to tetramethylsilane ($\delta = 0$ ppm). ^{31}P{^{1}H} NMR spectra were referenced externally to H_3PO_4 (85 %) ($\delta = 0$ ppm). Preparative flash column chromatography was conducted manually using glass columns packed with silica gel 60 (Merck, 40–63 μm).

High resolution-accurate mass data mass spectra were recorded on a hybrid Maxis Qq-aoTOF mass spectrometer (Bruker Daltonics, Bremen, Germany) fitted with an ESI-source. Measured accurate mass data of the $[M]^+$ ions for confirming calculated elemental compositions were typically within ±5 ppm accuracy. The mass calibration was done with a commercial mixture of perfluorinated trialkyl-triazines (ES Tuning Mix, Agilent Technologies, Santa Clara, CA, USA).

GC–MS analyses were conducted on a ISQ LT Single quadrupole MS (Thermo Fisher) directly interfaced to a TRACE 1300 Gas Chromatographic systems (Thermo Fisher), using a Rxi-5Sil MS (30 m, 0.25 mm ID) cross-bonded dimethyl polysiloxane capillary column at a carrier flow of He 1.5 mL/min.

General Procedure for Hydrogenation of Alkenes. Inside an argon flushed glovebox, a screw cap vial (8 mL) was charged with catalyst (2.2 mg, 5 μmol, 1 mol %), alkene (0.5 mmol, 1.0 equiv.) and solvent (0.5 mL). The vial was closed, transferred out of the glovebox and was flushed several times with hydrogen gas in an autoclave. It was subsequently put under hydrogen gas at a given pressure while stirring for a specified time at given temperature. Afterwards the reaction mixture was allowed to reach room temperature, depressurized and exposed to air to quench the catalyst. The sample (2 μL) was analyzed via GC-MS. After exposing the sample to air for 1 h, the solution was filtered through a thin pad of silica with diethylether. The solvent was then removed in *vacuo* to yield the pure product, which was characterized by ^{1}H- and ^{13}C{^{1}H} NMR spectroscopy. If purification was not possible, *n*-dodecane was added as standard to the GC-MS sample to determine the yield.

Syntheses. *fac*-[Mn(PC-*i*Pr)$(CO)_3(CH_2CH_2CH_3)$] (2). *fac*-[Mn(PC-*i*Pr)$(CO)_3$(**$CH_2CH_2CH_3$**) (**1**) (250 mg, 0.52 mmol, 1.0 equiv.) was dissolved in dry THF (15 mL) and Na (36 mg, 1.56 mmol, 3.0 equiv.) was added and the mixture was stirred at room temperature for 24 h. Then 1-bromopropane (639 mg, 5.20 mmol, 10 equiv.) was added and the solution was stirred for another 15 min. The solution was then decanted and the precipitate was extracted with *n*-pentane (7×20 mL). The combined organic phases were taken to dryness and the resulting orange powder was washed with cold *n*-pentane (3 mL) and dried, yielding 167 mg of **2** (73 %) as a beige solid. ^{1}H NMR (600 MHz, C_6D_6): $\delta = 6.98$–6.91 (m, 1H, aromatic CH), 6.91–6.85 (m, 1H, aromatic CH), 6.62 (d, $J = 7.8$ Hz, 1H, aromatic CH), 6.49 (d, $J = 8.0$ Hz, 1H, aromatic CH), 3.62 (s, 3H, N-CH_3), 3.51–3.39 (m, 2H, N-CH_2-P), 2.45–2.34 (m, 1H, P-CH(CH_3)), 2.10–1.99 (m, 1H, Mn-CH_2-CH_2-CH_3), 1.87–1.74 (m, 2H, P-CH(CH_3), superimposed by Mn-CH_2-CH_2-CH_3), 1.29 (q, $J = 7.3$ Hz, 3H, P-CH(CH_3)), 1.22 (t, $J = 7.1$ Hz, 3H, Mn-CH_2-CH_2-CH_3), 1.06 (dd, $J = 15.8$, 6.8 Hz, 3H, P-CH(CH_3)), 0.86 (dd, $J = 11.3$, 10.5 Hz, 3H, P-CH(CH_3)), 0.70–0.60 (m, 1H, Mn-CH_2-CH_2-CH_3), 0.44 (q, $J = 6.9$ Hz, 3H, P-CH(CH_3)), 0.38–0.28 (m, 1H, Mn-CH_2-CH_2-CH_3) ppm. ^{31}P{^{1}H} NMR (243 MHz, C_6D_6): $\delta = 104.6$ ppm. ^{13}C{^{1}H} NMR (151 MHz, C_6D_6): $\delta = 228.4$ (CO), 227.1 (CO), 222.7 (d, $J = 41.2$ Hz, N–C-N), 136.8 (aromatic C), 133.4 (d, $J = 7.2$ Hz, aromatic C), 122.2 (aromatic CH), 109.7 (aromatic CH), 109.2 (aromatic CH), 44.2 (N-CH_2-P), 44.1 (N-CH_2-P), 34.7 (N-CH_3), 30.6 (Mn-CH_2-CH_2-CH_3), 25.1 (P-CH(CH_3)), 25.0 (P-CH(CH_3)), 24.8 (P-CH(CH_3)), 24.7 (P-CH(CH_3)), 22.3 (Mn-CH_2-CH_2-CH_3), 19.9 (d, $J = 4.3$ Hz, P-CH(CH_3)), 18.8 (t, $J = 5.5$ Hz, P-CH(CH_3)), 18.7 (P-CH(CH_3)), 17.4 (d, $J = 1.7$ Hz, P-CH(CH_3)), 13.2 (Mn-CH_2-CH_2-CH_3), 13.1 (Mn-CH_2-CH_2-CH_3) ppm. IR (ATR, cm^{-1}): 1965 (CO), 1882 (CO), 1852 (CO). HR-MS: *m/z* calcd for $C_{18}H_{23}MnN_2O_3P$ $[M-C_3H_7]^+$ 401.0821, found 401.0821.

X-ray Structure Determination. Data of **1** (CSD 2352079) were collected at $T = 200$ K in a dry stream of nitrogen on a STOE STADIVARI diffractometer system equipped with a Dectris Eiger CdTe hybrid photon counting detector using Cu-$K\alpha$ radiation ($\lambda = 1.54186$ Å). X-ray diffraction data of **2** (CSD 2352080) were collected at $T = 100$ K in a dry stream of nitrogen on a Bruker Kappa APEX II diffractometer system using Mo-$K\alpha$ radiation ($\lambda = 0.71073$ Å). Data were reduced to intensity values with SAINT and an absorption correction was applied with the multi-scan approach implemented in SADABS.[18] Data were reduced with X-Area and an absorption correction was applied with the multi-scan approach implemented in LANA.[19] The structures were solved by the dual-space approach implemented in SHELXT[20] and refined against F^2 with SHELXL.[21] H atoms were placed at calculated positions and refined as riding on their parent atom. Molecular graphics were generated with the program MERCURY.[22]

Computational Details. Calculations were performed using the GAUSSIAN 09 software package[23] and the PBE0 functional, without symmetry constraints. That functional uses a hybrid generalized gradient approximation (GGA), including 25 % mixture of Hartree-Fock[24] exchange with DFT[17] exchange-correlation, given by Perdew, Burke and Ernzerhof functional (PBE).[25] The optimized geometries were obtained with the Stuttgart Effective Core Potentials and associated basis set (SDD)[26] for Mn, and a standard 6–31G(d,p)[27] for the remaining elements (basis b1). Transition state optimizations were performed with the Synchronous Transit-Guided Quasi-Newton Method (STQN) developed by Schlegel *et al*,[28] following extensive searches of the Potential Energy Surface. Frequency calculations were performed to confirm the nature of the stationary points, yielding one imaginary frequency for the transition states and none for the minima. Each transition state was further confirmed by following its vibrational mode downhill on both sides and obtaining the minima presented on the energy profile. Solvent effects (THF) were considered in *all* calculations (PBE0/b1 geometry optimizations included) using the Polarizable Continuum Model (PCM) initially devised by Tomasi and co-workers[29] with radii and non-electrostatic terms of the SMD solvation model, developed by Truhlar *et al.*[30] The electronic energies (E_{b1}) obtained at the PBE0/b1 level of theory were converted to free energy at 298.15 K and 1 atm (G_{b1}) by using zero point energy and thermal energy corrections based on structural and vibration frequency data calculated at the same level.

Supporting Information Summary

The authors have cited additional references within the Supporting Information,[18–37] which includes X-ray crystallographic data for **1** and **2** (CCDC 2352079 and 2352080) (CIF), synthetic procedures, ^{1}H, ^{13}C{^{1}H}, and ^{31}P{H} NMR spectra of all compounds, crystallographic data and complete computational details, and cartesian coordinates for DFT-optimized structures (XYZ).

Acknowledgements

Financial support by the Austrian Science Fund (FWF) is gratefully acknowledged (Project No. P 32570-N). LFV is grateful for the Fundação para a Ciência e a Tecnologia, I.P/; MCTES through national funds PIDDAC-CQE UIDB/00100/2020 and UIDP/00100/2020 (DOI 10.54499/UIDP/00100/2020). And IMS the Associated Laboratory funded by Project LA/P/0056/2020 (DOI 10.54499/LA/P/0056/2020).

Conflict of Interests

The authors declare no conflict of interests.

Data Availability Statement

The data that support the findings of this study are available from the corresponding author upon reasonable request.

Keywords: Manganese · Alkenes · Hydrogenation · NHC phosphine · DFT calculations

[1] *Catalysis Without Precious Metals* (Ed: R. M. Bullock), Wiley-VCH, Weinheim **2010**.

[2] H.-U. Blaser, F. Spindler, M. Thommen, In *The Handbook of Homogeneous Hydrogenation* (Eds: J. G. de Vries, C. J. Elsevier) Wiley-VCH, Weinheim **2008** Chapter 37, 1279–1324.

[3] T. N. Gieshoff, A. Jakobi von Wangelin In *Non-Noble Metal Catalysis: Molecular Approaches and Reactions* (Eds: R. J. M. Klein Gebbink, M.-E. Moret) Wiley-VCH, Weinheim **2019** Chapter 5, pp 97–126.

[4] L. C. M. Castro, H. Li, J.-B. Sortais, C. Darcel, *Green Chem.* **2015**, *17*, 2283–2303.

[5] a) I. Bauer, H.-J. Knölker, *Chem. Rev.* **2015**, *115*, 3170–3387; b) A. Fürstner, *ACS Cent. Sci.* **2016**, *2*, 778–789

[6] T. Zell, D. Milstein, *Acc. Chem. Res.* **2015**, *48*, 1979–1994.

[7] S. Chakraborty, P. Bhattacharya, H. Dai, H. Guan, *Acc. Chem. Res.* **2015**, *48*, 1995–2003.

[8] a) P. J. Chirik, *Acc. Chem. Res.* **2015**, *48*, 1687–1695; b) R. Arevalo, P. J. Chirik, *J. Am. Chem. Soc.* **2019**, *141*, 9106–9123.

[9] For recent examples of iron, cobalt, and nickel catalyzed olefin hydrogenations, see: a) L. J. Murphy, M. J. Ferguson, R. McDonald, M. D. Lumsden, L. Turculet, *Organometallics* **2018**, *37*, 4814–4826; b) Y. Sunada, H. Ogushi, T. Yamamoto, S. Uto, M. Sawano, A. Tahara, H. Tanaka, Y. Shiota, K. Yoshizawa, H. Nagashima, *J. Am. Chem. Soc.* **2018**, *140*, 4119–4134; c) R. Xu, S. Chakraborty, S. M. H. Bellows, T. R. Cundari, W. D. Jones, *ACS Catal.* **2016**, *6*, 2127–2135; d) M. R. Friedfeld, M. Shevlin, G. W. Margulieux, L.-C. Campeau, P. J. Chirik, *J. Am. Chem. Soc.* **2016**, *138*, 3314–3324; e) K. Tokmic, C. R. Markus, L. Zhu, A. R. Fout, *J. Am. Chem. Soc.* **2016**, *138*, 11907–11913; f) S. Sandl, T. M. Maier, N. P. van Leest, S. Kröncke, U. Chakraborty, S. Demeshko, K. Koszinowski, B. de Bruin, F. Meyer, M. Bodensteiner, C. Herrmann, R. Wolf, A. Jacobi von Wangelin, *ACS Catal.* **2019**, *98*, 7596–7606; g) Y. Wang, A. Kostenko, S. Yao, M. Driess, *J. Am. Chem. Soc.* **2017**, *139*, 13499–13506; h) N. G. Léonard, P. J. Chirik, *ACS Catal.* **2018**, *8*, 342–348; i) H. Wei, H. Chen, J. Chen, I. D. Gridnev, W. Zhang, *Angew. Chem. Int. Ed.* **2023**, *62*, e202214990; j) P. Viereck, S. M. Rummelt, N. A. Soja, T. P. Pabst, P. J. Chirik, *Organometallics* **2021**, *40*, 1053–1061; k) M.-P. Lücke, S. Yao, M. Driess, *Chem. Sci.* **2021**, *12*, 2909–2915; l) P. Lu, H. Wang, Y. Mao, X. Hong, Z. Lu, *J. Am. Chem. Soc.* **2022**, *144*, 17359–17364; m) P. Lu, X. Ren, H. Xu, D. Lu, Y. Sun, Z. Lu, *J. Am. Chem. Soc.* **2021**, *143*, 12433–12438; n) S. Chakrabortty, K. Konieczny, F. J. de Zwart, E. O. Bobylev, E. Baráth, S. Tin, B. H. Müller, J. N. H. Reek, B. de Bruin, J. G. de Vries, *Angew. Chem. Int. Ed.* **2023**, *62*, e202301329.

[10] For recent reviews and book chapters on manganese-based (de)hydrogenation and related reactions see: a) K. Das, S. Waiba, A. Jana, B. Maji, *Chem. Soc. Rev.* **2022**, *51*, 4386–4464; b) P. Schlichter, C. Werlé, *Synthesis* **2022**, *54*, 517–534; c) S. Weber, K. Kirchner, *Acc. Chem. Res.* **2022**, *55*, 2740–2751; d) Y. Wang, M. Wang, Y. Li, Q. Liu, *Chem* **2021**, *7*, 1180–1223; e) A. Mukherjee, D. Milstein, *ACS Catal.* **2018**, *8*, 11435–11469; f) F. Kallmeier, R. Kempe, *Angew. Chem. Int. Ed.* **2018**, *57*, 46–60; g) G. A. Filonenko, R. van Putten, E. J. M. Hensen, E. A. Pidko, *Chem. Soc. Rev.* **2018**, *47*, 1484–1515; h) N. Gorgas, K. Kirchner, *Acc. Chem. Res.* **2018**, *51*, 1558–1569; i) M. Garbe, K. Junge, M. Beller, *Eur. J. Org. Chem.* **2017**, 4344–4362; j) B. Maji, M. Barman, *Synthesis* **2017**, *49*, 3377–3393; k) Y. Wang, Q. Liu, *Synlett* **2020**, *31*, 1464–1473; l) L. Alig, M. Fritz, S. Schneider, *Chem. Rev.* **2019**, *119*, 2681–2751; m) V. Papa, J. Fessler, F. Zaccaria, J. Hervochon, P. Dam, C. Kubis, A. Spannenberg, Z. Wei, H. Jiao, C. Zuccaccia, A. Macchioni, K. Junge, M. Beller, *Chem. Eur. J.* **2023**, *29*, e202202774; n) J. Yang, L. Yao, Z. Wang, Z. Zuo, S. Liu, P. Gao, M. Han, Q. Liu, G. A. Solan, W.-H. Sun, *J. Catal.* **2023**, *418*, 40–50; o) Z. Wei, H. Li, Y. Wang, Q. Liu, *Angew. Chem. Int. Ed.* **2023**, *62*, e202301042; p) K. Azouzi, L. Pedussaut, R. Pointis, A. Bonfiglio, R. Kumari Riddhi, C. Duhayon, S. Bastin, J.-B. Sortais, *Organometallics* **2023**, *42*, 1832–1838; q) C. L. Oates, A. S. Goodfellow, M. Bühl, M. L. Clarke, *Angew. Chem. Int. Ed.* **2023**, *62*, e202212479; r) K. Azouzi, R. Pointis, R. Buhaibeh, P. H. Fernández, L. Pedussaut, M. Boundor, A. Bonfiglio, A. Bruneau-Voisine,

D. Wei, T. Roisnel, C. Duhayon, M. Á. Casado, D. A. Valyaev, Y. Canac, S. Bastin, C. Raynaud, J.-B. Sortais, *J. Catal.* **2024**, *430*, 115334; s) K. Dey, G. de Ruiter, *Org. Lett.* **2024**, *26*, 4173–4177.

[11] a) S. Weber, B. Stöger, K. Kirchner, *Org. Lett.* **2018**, *20*, 7212–7215; b) S. Weber, L. F. Veiros, K. Kirchner, *Adv. Synth. Catal.* **2019**, *361*, 5412–5420; c) S. Weber, B. Stöger, L. F. Veiros, K. Kirchner, *ACS Catal.* **2019**, *9*, 9715–9720; d) S. Weber, J. Brünig, L. F. Veiros, K. Kirchner, *Organometallics* **2021**, *40*, 1388–1394; e) S. Kostera, S. Weber, M. Peruzzini, L. F. Veiros, K. Kirchner, L. Gonsalvi, *Organometallics* **2021**, *40*, 1213–1220; f) D. P. Zobernig, M. Luxner, B. Stöger, L. F. Veiros, K. Kirchner, *Chem. Eur. J.* **2024**, *30*, e202302455; g) R. A. Farrar-Tobar, S. Weber, Z. Csendes, A. Ammaturo, S. Fleissner, H. Hoffmann, L. F. Veiros, K. Kirchner, *ACS Catal.* **2022**, *12*, 2253–2260.

[12] a) U. Chakraborty, E. Reyes-Rodriguez, S. Demeshko, F. Meyer, A. Jacobi von Wangelin, *Angew. Chem. Int. Ed.* **2018**, *57*, 4970–4975; b) U. Chakraborty, S. Demeshko, F. Meyer, A. Jacobi von Wangelin, *Angew. Chem. Int. Ed.* **2019**, *58*, 3466–3470.

[13] S. M. W. Rahaman, D. K. Pandey, O. Rivada-Wheelaghan, A. Dubey, R. R. Fayzullin, J. R. Khusnutdinova, *ChemCatChem* **2020**, *12*, 5912–5918.

[14] N. F. Both, A. Spannenberg, H. Jiao, K. Junge, M. Beller, *Angew. Chem. Int. Ed.* **2023**, *135*, e202307987.

[15] D. P. Zobernig, M. Luxner, B. Stöger, L. F. Veiros, K. Kirchner, *Chem. Eur. J.* **2024**, *30*, e202302455.

[16] D. P. Zobernig, B. Stöger, L. F. Veiros, K. Kirchner, *ACS Catal.* **2024**, *14*, 12385–12391.

[17] a) R. G. Parr, W. Yang, *Density Functional Theory of Atoms and Molecules*, Oxford University Press, New York **1989**; b) Free energy values were obtained at the PBE0/(SDD,6-31G(d,p)) level using the Gaussian 09 package. Calculations included solvent effects (THF) using the PCM/SMD model. A full account of the computational details and a complete list of references are provided in the supporting information.

[18] Bruker computer programs: APEX3, SAINT and SADABS (Bruker AXS Inc., Madison, WI **2020**.

[19] X-Area 1.31.175.0, LANA 2.6.2.0 (STOE & Cie GmbH, Darmstadt, Germany, **2021**).

[20] G. M. Sheldrick, *Acta Crystallogr.* **2015**, *A71*, 3–8.

[21] G. M. Sheldrick, *Acta Crystallogr.* **2015**, *C71*, 3–8.

[22] C. F. Macrae, P. R. Edgington, P. McCabe, E. Pidcock, G. P. Shields, R. Taylor, M. Towler, J. van de Streek, *J. Appl. Crystallogr.* **2006**, *39*, 453–457.

[23] Gaussian, 09, Revision, **A.01**, M. J. Frisch, G. W. Trucks, H. B. Schlegel, G. E. Scuseria, M. A. Robb, J. R. Cheeseman, G. Scalmani, V. Barone, B. Mennucci, G. A. Petersson, H. Nakatsuji, M. Caricato, X. Li, H. P. Hratchian, A. F. Izmaylov, J. Bloino, G. Zheng, J. L. Sonnenberg, M. Hada, M. Ehara, K. Toyota, R. Fukuda, J. Hasegawa, M. Ishida, T. Nakajima, Y. Honda, O. Kitao, H. Nakai, T. Vreven, J. A. Montgomery Jr., J. E. Peralta, F. Ogliaro, M. Bearpark, J. J. Heyd, E. Brothers, K. N. Kudin, V. N. Staroverov, R. Kobayashi, J. Normand, K. Raghavachari, A. Rendell, J. C. Burant, S. S. Iyengar, J. Tomasi, M. Cossi, N. Rega, J. M. Millam, M. Klene, J. E. Knox, J. B. Cross, V. Bakken, C. Adamo, J. Jaramillo, R. Gomperts, R. E. Stratmann, O. Yazyev, A. J. Austin, R. Cammi, C. Pomelli, J. W. Ochterski, R. L. Martin, K. Morokuma, V. G. Zakrzewski, G. A. Voth, P. Salvador, J. J. Dannenberg, S. Dapprich, A. D. Daniels, Ö. Farkas, J. B. Foresman, J. V. Ortiz, J. Cioslowski, D. J. Fox, Gaussian, Inc., Wallingford CT **2009**.

[24] W. J. Hehre, L. Radom, P. R. Schleyer, J. A. Pople, *Ab Initio Molecular Orbital Theory*, John Wiley & Sons, NY **1986**.

[25] a) J. P. Perdew, K. Burke, M. Ernzerhof, *Phys. Rev. Lett.* **1996**, *77*, 3865–3868; b) J. P. Perdew, K. Burke, M. Ernzerhof, *Phys. Rev. Lett.* **1997**, *78*, 1396–1396; c) J. P. Perdew, *Phys. Rev. B* **1986**, *33*, 8822–8824.

[26] a) U. Haeusermann, M. Dolg, H. Stoll, H. Preuss, P. Schwerdtfeger, R. M. Pitzer, *Mol. Phys.* **1993**, *78*, 1211–1224; b) W. Kuechle, M. Dolg, H. Stoll, H. Preuss, *J. Chem. Phys.* **1994**, *100*, 7535–7542; c) T. Leininger, A. Nicklass, H. Stoll, M. Dolg, P. Schwerdtfeger, *J. Chem. Phys.* **1996**, *105*, 1052–1059.

[27] a) R. Ditchfield, W. J. Hehre, J. A. Pople, *J. Chem. Phys.* **1971**, *54*, 724–728; b) W. J. Hehre, R. Ditchfield, J. A. Pople, *J. Chem. Phys.* **1972**, *56*, 2257–2261; c) P. C. Hariharan, J. A. Pople, *Mol. Phys.* **1974**, *27*, 209–214; d) M. S. Gordon, *Chem. Phys. Lett.* **1980**, *76*, 163–168; e) P. C. Hariharan, J. A. Pople, *Theor. Chim. Acta* **1973**, *28*, 213–222.

[28] a) C. Peng, P. Y. Ayala, H. B. Schlegel, M. J. Frisch, *J. Comb. Chem.* **1996**, *17*, 49–56; b) C. Peng, H. B. Schlegel, *Isr. J. Chem.* **1993**, *33*, 449–454.

[29] a) M. T. Cancès, B. Mennucci, J. A. Tomasi, *J. Chem. Phys.* **1997**, *107*, 3032–3041; b) M. Cossi, V. Barone, B. Mennucci, J. Tomasi, *Chem. Phys. Lett.* **1998**, *286*, 253–260; c) B. Mennucci, J. Tomasi, *J. Chem. Phys.* **1997**, *106*, 5151–5158; d) J. Tomasi, B. Mennucci, R. Cammi, *Chem. Rev.* **2005**, *105*, 2999–3094.

[30] A. V. Marenich, C. J. Cramer, D. G. Truhlar, *J. Phys. Chem. B* **2009**, *113*, 6378–6396.

[31] D. J. Frank, L. Guiet, A. Käslin, E. Murphy, S. P. Thomas, *RSC Adv.* **2013**, *3*, 25698–25701.

[32] S. P. Cummings, T.-N. Le, G. E. Fernandez, L. G. Quiambao, B. J. Stokes, *J. Am. Chem. Soc.* **2016**, *138*, 6107–6110.

[33] B. Pieber, T. Glasnov, C. O. Kappe, *Chem. Eur. J.* **2015**, *21*, 4368–4376.

[34] T. Liu, Y. Zeng, H. Zhang, T. Wei, X. Wu, N. Li, *Tetrahedron Lett.* **2016**, *57*, 4845–4849.

[35] C. Zheng, S. Pu, J. Xu, M. Luo, D. Huang, L. Shen, *Tetrahedron* **2007**, *63*, 5437–5449.

[36] Y. Imada, M. Osaki, M. Noguchi, T. Maeda, M. Fujiki, S. Kawamorita, N. Komiya, T. Naota, *ChemCatChem* **2015**, *7*, 99–106.

[37] K. Ganguli, S. Shee, D. Panja, S. Kundu, *Dalton Trans.* **2019**, *48*, 7358–7366.

Manuscript received: July 3, 2024
Revised manuscript received: August 8, 2024
Accepted manuscript online: August 10, 2024
Version of record online: October 24, 2024